Influence of Route of Administration and Lipidation of Apolipoprotein A-I Peptide on Pharmacokinetics and Cholesterol Mobilization

Jie Tang[1], Dan Li[1], Lindsey Drake[2], Wenmin Yuan[1], Sara Deschaine[1], Emily E. Morin[1], Rose Ackermann[1], Karl Olsen[1], David E. Smith[1], Anna Schwendeman[1,3,*]

[1]*Department of Pharmaceutical Sciences, College of Pharmacy, University of Michigan, 428 Church Street, Ann Arbor, MI 48109*

[2]*Department of Medicinal Chemistry, College of Pharmacy, University of Michigan, 428 Church Street, Ann Arbor, MI 48109*

[3]*Biointerfaces Institute, University of Michigan, NCRC, 2800 Plymouth Road, Ann Arbor, MI 48109*

[*]Corresponding author

E-mail address: annaschw@med.umich.edu

Phone: +1 734 763 4056

Fax: +1 734 615 6162

Running title: ApoA-I peptide lipidation/administration route affect PK-PD

Abbreviations: ApoA-I, apoliprotein A-I; IV, intravenous; IP, intra-peritoneal; 22A/ESP24218, apoA-I mimetic peptide consisting of 22 amino acids–PVLDLFRELLNELLEALKQKLK; 5A, apoA-I mimetic peptide consisting of 37 amino acids–DWLKAFYDKVAEKLKEAFPDWAKAAYDKAAEKAKEAA; 22A-sHDL, phospholipid reconstituted HDL based on 22A; DPPC, 1,2-dipalmitoyl-sn-glycero-3-phosphocholine; HDL-C, HDL cholesterol; PK, Pharmacokinetic; PD, pharmacodynamic; GPC, gel permeation chromatography; DLS, dynamic light scattering; IS, internal standard; EIC, extracted ion chromatogram; TIC, total ion chromatogram; PL, phospholipids; TC, total cholesterol; FC, unesterified or free cholesterol; CE, cholesterol ester; RCT, reverse cholesterol transport.

Abstract

Apoliprotein A-I (apoA-I), apoA-I mimetic peptides and their lipid complexes or reconstituted high-density lipoprotein (HDL) have been studied as treatments for various pathologies. However, consensus is lacking about the best method for administration - by intravenous (IV) or intra-peritoneal (IP) routes, and formulation - as an HDL particle or in a lipid-free form. The objective of this study was to systematically examine peptide plasma levels, cholesterol mobilization and lipoprotein remodeling *in vivo* following administration of lipid-free apoA-I peptide (22A) or phospholipid reconstituted 22A-sHDL by IV and IP routes. The mean circulation half-life was longer for 22A-sHDL ($T_{1/2}$ = 6.27 h) than for free 22A ($T_{1/2}$ = 3.81 h). The percent of 22A absorbed by the vascular compartment after the IP dosing was ~50% for both 22A and 22A-sHDL. The strongest pharmacologic response came from IV injection of 22A-sHDL - specifically a 5.3-fold transient increase in plasma free cholesterol (FC) level compared to 1.3 and 1.8-fold FC increases for 22A-IV and 22A-sHDL-IP groups. Addition of either 22A or 22A-sHDL to rat plasma caused lipoprotein remodeling and appearance of a lipid poor apoA-I. Hence, both the route of administration and the formulation of apoA-I peptide significantly affect its pharmacokinetics and pharmacodynamics.

Key words

Apolipoproteins; Cholesterol; HDL; Lipoproteins/Metabolism; Pharmacokinetics; Apolipoprotein A-I mimetic peptides; Lipoprotein remodeling; PK-PD modeling

Introduction

The therapeutic use of apolipoprotein A-I (apoA-I), its mutants, and peptide mimetics for the treatment of atherosclerosis has been studied in a variety of animal models and clinical trials (1, 2). However, there is a lack of consensus regarding whether the apoA-I protein or peptide should be administered in a lipid-free form or bound to phospholipids as a reconstituted HDL particle. Early clinical trials showed that infusion of lipid-free apoA-I failed to increase circulation level of HDL cholesterol (HDL-C) and resulted in shorter circulation time than that for endogenous apoA-I (3). Consequently, the majority of clinically developed apoA-I products have been administered as reconstituted HDL particles: apoA-I/soybean phosphatidylcholine (CSL-111 and CSL-112), apoA-I-Milano/palmitoyl-oleoyl-phosphotidylcholine (ETC-216), and apoA-I/sphingomyelin/dipalmitoyl-phosphorylglycerol (CER-001) (2, 4, 5). In contrast, many preclinical studies have been performed using infusions of lipid-free proteins, and apoA-I peptides have been optimized for their pharmacological activity in lipid-free form (6).

There is also an uncertainty concerning the mechanism(s) by which reconstituted HDL infusions elicit pharmacological effects and whether such mechanism(s) differ(s) from that used by lipid-free apoA-I. The ability of lipid-free apoA-I to efflux lipids through interaction with the ATP-binding cassette transporter (ABCA1) and its capacity to form de novo functional pre-β HDL particles are considered to be critical for cholesterol efflux *in vivo* (7, 8). However, infused apoA-I peptides or proteins do not remain in the lipid-free form. Rather, they bind and remodel endogenous HDL, improving its functionality and thereby eliciting a pharmacological effect (9, 10). In contrast, when apoA-I is dosed in the form of an HDL particle, the magnitude of its pharmacological effect, measured by the degree of cholesterol mobilization from tissues to plasma, depends on the HDL's phospholipid composition (11, 12).

In a similar fashion, there is a lack of consensus surrounding the optimal route of administration for apoA-I and its mimetic peptides. For long term dosing in rodents,

intraperitoneal (IP) administration is preferred for a technical reason, namely the difficulty of repeated dosing in the tail vein (13). However, in many acute studies, apoA-I and HDL are administered intravenously (IV) specifically because these compounds act in the vascular compartment through either remodeling endogenous lipoproteins or direct efflux of the excess of cholesterol from foam cells in atheroma (14, 15). The effective dose of apoA-I or reconstituted HDL that reaches circulation is likely lower following IP administration in comparison to IV administration due to loss occurring during absorption from tissue to the vascular compartment. Yet, the fraction of apoA-I or HDL that is actually capable of reaching the vasculature following IP dose has not been experimentally determined yet.

With growing interest around the potential therapeutic roles of administered reconstituted HDL and apoA-I in the treatment of sepsis, diabetes, rheumatoid arthritis, lupus, and other diseases (11, 16, 17), it is important to develop a basic understanding of HDL/apoA-I pharmacokinetics in order to select the proper dose, dosing intervals, and route of administration. In addition, the ability to measure basic HDL-related biomarkers of pharmacological effect in order to understand how these biomarkers relate to the dose, dosing interval, and administration route is important. Having this information at hand will allow investigators to select pharmacologically relevant doses and avoid obtaining false negative results. Pharmacokinetic-pharmacodynamic (PK/PD) modeling is a scientific tool to relate PK models (describing the relationship between dose, systemic drug exposure and time) to PD models (describing the mathematical relationship between exposure level and the pharmacological effect) (18). By establishing PK/PD modeling, the relationship between the PK and PD profile can be quantified, providing an assessment of effect onset/duration relative to the plasma PK profile (19).

In this study, we selected a "two by two" experimental design to compare the administration of apoA-I peptide and apoA-I peptide reconstituted HDL following IV and IP administrations in normal adult male rats. We selected the synthetic peptide 22A, or ESP24218, as a model apoA-I mimetic peptide. This peptide was the first apoA-I mimetic peptide to reach clinical development,

which has been administered clinically in both single and multiple-dose trials, and its human pharmacokinetic data is available (20, 21). We determined peptide and phospholipid pharmacokinetics and measured cholesterol mobilization in plasma, distribution of mobilized cholesterol among HDL, low-density lipoprotein (LDL), and very-low-density lipoprotein (VLDL) particles, plasma efflux capacity, and lipoprotein remodeling following free 22A and 22A reconstituted HDL dosing.

2. Materials and Methods

2.1 Materials

ApoA-I mimetic peptides 22A, PVLDLFRELLNELLEALKQKLK, and 5A, DWLKAFYDKVAEKLKEAFPDWAKAAYDKAAEKAKEAA, were synthesized by Genscript Inc. (Piscataway, NJ). The purities of peptides were determined to be over 95% by reserve phase HPLC. Phospholipids 1-palmitoyl-2-oleoyl-*sn*-glycero-3-phosphocholine (POPC) and 1,2-dipalmitoyl-*sn*-glycero-3-phosphocholine (DPPC) were generously donated by Nippon Oils and Fats (Osaka, Japan). All other materials were obtained from commercial sources.

2.2 Preparation and characterization of 22A-sHDL particles

Synthetic HDL particles were prepared by the thin film-hydration method. Briefly, DPPC and POPC were dissolved in chloroform at 20 mg/mL. 22A peptide was dissolved in methanol: water (1:1 volume ratio) at 10 mg/mL. DPPC, POPC, and 22A were mixed in a 4 mL glass vial at different weight ratios and vortexed for 5 s. The mixture was dried by nitrogen gas flow and then placed in the vacuum oven overnight to remove residual solvent. The resulting lipid film was hydrated with PBS (pH 7.4) (final concentration of 22A = 15 mg/mL) and vortexed. The suspension was homogenized in a bath sonicator for 5 min and then with a probe sonicator intermittently (50 W×10 S×12 cycles) to form a clear or translucent 22A-sHDL solution.

2.3 Analysis of 22A-sHDL particles

The purity of 22A-sHDL was analyzed by gel permeation chromatography (GPC) with UV detection at 220 nm using Tosoh TSK gel G3000SWx 7.8mm x 30cm column (Tosoh Bioscience, King of Prussia, PA) on a Waters Breeze Dual Pump system. The HDL samples were diluted to 1 mg/mL peptide concentration and an injection volume of 10 μL was used. The samples were eluted with PBS (pH 7.4) at a flow rate of 1 mL/min. The sHDL hydrodynamic diameters were

determined by dynamic light scattering (DLS), using a Zetasizer Nano ZSP, Malvern Instruments (Westborough, MA). Samples were diluted to 1.5 mg/mL peptide concentration. The volume intensity average values were reported.

2.4 Rat pharmacokinetics and cholesterol mobilization

Male Sprague-Dawley rats (300 ~ 350 mg) were purchased from Charles River Laboratories (Wilmington, MA) and acclimated for one week. The animals were maintained on a chow diet. Prior to dosing, the animals were fasted overnight and received either 22A peptide or 22A-sHDL particles at 75 mg/kg by either intraperitoneal (IP) or intravenous injection (IV). Four groups of rats (n = 4/group) were dosed as follows: IV dose of 22A solution group; IP dose of 22A solution group; IV dose of 22A-sHDL group and IP dose of 22A-sHDL group. Blood (300 - 500 µL) was drawn from the jugular vein into BD microtainer (TM) tubes (BD, Franklin Lakes, NJ) for capillary blood collection at pre-dose and 0.25, 0.5, 1, 2, 4, 8 and 24 after dosing. The animals were fed following the 8 h time-point and fasted again prior to the 24 h bleed. Serum was isolated immediately from the whole blood by centrifugation at 14,000 rpm for 10 min at 4 °C. Serum was aliquoted into multiple tubes and stored at -80°C prior to analysis.

2.5 LC-MS analysis of peptide plasma levels

Immediately after serum separation, 10 µL of 5A peptide (3 mg/mL) was added to 10 µL of serum as an internal standard (IS), peptides were extracted with 100 µL of methanol containing 0.1% acetic acid. After vortexing for 30 s, the mixture was centrifuged at 14,000 rpm for 10 min at 4°C. The top layer was drawn off and used for quantifying peptide levels in the serum, using Agilent 6520 Accurate-Mass Q-TOF LC/MS equipped with a dual electrospray ionization source (Dual-ESI) (Agilent Technologies, CA). The HPLC separation was performed using the Agilent 300SB-C18 column (2.1 mm × 50 mm, 3.5 µm). The mobile phase consisted of (A) water containing 0.1% (v:v) formic acid and (B) methanol (pH 2.2) containing 0.1% (v:v) formic acid

using a gradient elution of 10% to 60% B at 0-3.5 min, and 60% to 95% B at 3.5-8 min. The flow rate was 0.4 mL/min with an injection volume of 10 μL. Mass spectra were acquired in negative ion mode with the mass range set at m/z 100-3200. The conditions used for the ESI source included a capillary voltage of 3500 V, a drying gas temperature of 332 °C, a drying gas flow of 5 L/min, and a nebulizer pressure of 45 psi as well as a fragmentor voltage of 225 V. MassHunter Workstation software (Agilent Technologies, CA) was used for data acquisition and processing. The extracted ion chromatogram (EIC) of 22A was exported from the total ion chromatogram (TIC) by monitoring the key fragment of 22A at m/z 656.6. Analogously, the EIC of 22A (-)Lys metabolite and IS 5A was extracted at m/z 832.5 and m/z 844.4, respectively. The total integral area of 22A peak and 22A (-)Lys metabolite peak was used to calculate concentration.

2.6 Measurement of plasma lipids

The levels of serum phospholipids (PL), total cholesterol (TC), and unesterified or free cholesterol (FC) were determined by enzymatic analysis using commercially available kits (Wako Chemicals, Richmond, VA). The cholesterol ester level (CE) was calculated as the difference between TC and FC levels at each time point. Briefly, serum samples were diluted with PBS (pH 7.4) 10-fold for TC detection and 3 fold for FC detection and with Milli Q water 10 times for PL detection. Defined amounts of standards or diluted samples were transferred into 96-well plate (50 μL, 60 μL and 20 μL for TC, FC and PL, respectively). Color reagents were added according to manufacturer instructions. The plates were gently shaken using an orbital shaker and incubated at 37 ˚C for 5 min The UV absorbance at 600 nm was measured by a Synergy NEO HTS Multi-Mode Microplate Reader (Bio-Tek).

2.7 Pharmacokinetic parameters calculation and PK-PD modeling

Pharmacokinetic (PK) and pharmacodynamic (PD) analyses of the data were performed by least-squares regression analysis, weighted by the inverse of the fitted value, using Phoenix©

WinNonlin® (Pharsight Corporation, Mountain View, CA, USA). Serum 22A and phospholipids (PL) PK parameters were estimated using a one-compartment disposition model for IV bolus administration, and a one-compartment disposition model with first order absorption and no lag time for IP administration. The PK parameters included time to reach maximum serum concentration (T_{max}), maximum serum concentration (C_{max}), area under the serum concentration-time curve (AUC), first-order absorption rate constant after IP injection (k_{01}), first-order elimination rate constant (k_{10}), elimination half-life ($T_{1/2}$), apparent total clearance (CL or CL/F, where F is bioavailabiliy) and apparent volume of distribution (V_d or Vd/F). The goodness of fit was determined using Akaike Information Criterion (AIC), and by visual inspection of the fits and residuals. The coefficient of variation (%CV) for each fitted parameter was also reported. The resulting pharmacokinetic parameters of 22A or phospholipids were then used as constants in the integrated PK-PD model.

The PK-PD model was established by relating serum concentrations of either 22A or the phospholipid components of 22A-sHDL to FC levels as the PD endpoint using indirect pharmacodynamic response models (19). Fig. 1 shows the indirect response model described by Jusko *et al*. for PK-PD modeling in this study (22). The pharmacologic response (free cholesterol mobilization) is controlled by a zero order rate constant for generation of response (k_{in}) and a first order rate constant for loss of response (k_{out}). The response compartment can be modulated by stimulating k_{in} using a sigmoidal infinite model. Steepness of the sigmoidal curve (γ) and the serum concentration needed to achieve a 50% maximum stimulation of response of a dosed agent (EC_{50}) were calculated. After the PK parameters were obtained by fitting to compartmental models, they were regarded as fixed values and then used to estimate PD parameters (i.e. k_{in}, k_{out}, EC_{50} *and* γ). The final models were chosen based on best fit in terms of sum of squared residuals, diagnosis plots and Log-likelihood value.

2.8 Distribution of mobilized cholesterol in lipoproteins

The rat sera samples were analyzed to assess cholesterol distribution between VLDL, LDL, and HDL lipoprotein fractions. Separation of lipoproteins was performed on Waters HPLC system equipped with Superose 6, 10/300 GL column (GE Healthcare, Piscataway, NJ) and on-line detection of cholesterol by post-column enzymatic reactions (23). Rat sera prior to dosing, 0.25, 2 and 24 h post-injection were analyzed. Sera aliquots (50 µl) were injected and eluted with a 154 mM sodium chloride/0.02% sodium azide solution at 0.8 ml/min. The post column reaction was done using a 5 mL reaction coil at 37°C and detected by UV at 490 nm. The cholesterol detection enzymatic reagents were delivered at 0.2 ml/min flow rate and mix-in with separated lipoprotein post column. The enzymatic reagent solution was composed of 100 mM phosphate buffer (pH 7.0), 4 M sodium chloride, 0.2% triton X-100, 10 mM sodium cholate, 2.5 mM 4-aminoantipyrine, 7.54 mM 2-hydroxy-3,5 dichlorobenzene, 0.0625 U/ml cholesterol oxidase, 1.25 U/ml peroxidase, 1.25 U/ml lipase and 0.1U/ml cholesterol ester hydrolase. All enzymatic reagents were purchased from Sigma.

2.9 Remodeling of endogenous plasma lipoprotein by lipid-free peptide and HDL particles

Remodeling of endogenous lipoproteins in serum was assessed after incubation of 22A peptide or 22A-sHDL with human sera. Solutions of 22A peptide or 22A-sHDL at 0.1, 0.5, 1.5 and 3 mg/mL peptide concentration in sera were incubated at 37°C for 1 h with shaking at 300 rpm. The various sub-classes of HDL were separated by size and charge by one-dimensional native polyacrylamide gel electrophoresis (PAGE) and visualized by western blot. Samples were subjected to electrophoresis using 10-well Tris-Borate-EDTA gradient (3-25%) acrylamide native gels (Jule, Inc., Milford, CT) (24). For each well, 5 µl of human sera after incubation with PBS, 22A peptide or 22A-sHDL was mixed with 5 µl of 2X TBE sample buffer and 6 µl of the resulting mixtures were loaded per well. Gels were run at 200 V until the sample dye was 2.5 cm away from the bottom of the gel. Proteins were visualized by western blot by transfer onto PVDF membrane and incubation overnight with anti-human apoA-I -HRP conjugated antibody

(Meridian Life Science, Memphis, TN). Bands were visualized using SuperSignal™ West Pico Chemiluminescence Substrate (Thermo Fisher) and images were acquired on a FluorChem M Imager (Protein Simple, San Jose, CA) and Image J was used for spot densitometry.

2.10 Statistical analyses

Statistical analyses of the data were performed by Student's t-test for comparing two treatment groups or by one-way ANOVA/Dunnett's test for comparing multiple treatment groups with 22A-sHDL/IV serving as the control. Data are expressed as mean ± standard deviation of at least three independent experiments. $P < 0.05$ was considered to be statistically significant.

3. Results

3.1 Composition optimization, assembly and characterization of 22A-sHDL particles

HDL composition was optimized using an apoA-I mimetic peptide, 22A, and phospholipids to match the size of endogenous pre-β HDL particles. The 22A peptide was previously clinically tested in dyslipidemia patients as ETC-642 (25). The composition of ETC-642 is approximately 1:1:1 weight ratios of 22A peptide, DPPC and sphingomyelin, combined to form homogeneous pre-β HDL-like discs (25). In this study we replaced sphingomyelin with POPC in order to increase sHDL interaction with lecithin-cholesteryl acyltransferase (LCAT). Unsaturated phospholipids like POPC are preferred substrates for LCAT, while sphingomyelin is not a substrate of the enzyme (26). In order to optimize 22A-sHDL particle size and purity, we varied the weight ratio of 22A to total phospholipids varied between 1:0.5 to 1:4 (Table 1). Gel permeation chromatography was used to examine the purity and the size distributions of newly generated 22A-sHDL particles. As shown in Fig. 2A, the retention times of different 22A-sHDL particles were between 7 and 10 min, the peak of unbound or lipid-free peptide appeared at around 11.5 min. The amount of lipid-free peptide was less than 0.48% for all formulations. The retention time of sHDL decreased with the increase of lipid to peptide ratio, indicating formation of larger sHDL particles.

Dynamic light scattering (DLS) analysis confirmed the increase of particle size from 5.5 nm to 12.5 nm with the increase of lipid:peptide ratio (Fig. 2B), which was consistent with the GPC results. The particle polydispersity index (PDI) for 0.5:1, 1:1 and 4:1 formulations were high, indicating heterogeneity of particle size (Table 1). Large PDI and small size for 0.5:1 and 1:1 formulation indicates insufficient amount of lipids for complete peptide binding and perhaps presence of peptide aggregates in the solution (27). Increasing the ratio to 4:1 resulted in larger PDI as well, indicating the presence of large lipid vehicles due to phospholipid excess. The

optimal lipid to peptide weight ratio for 22A peptide appears to be between 2:1 and 3:1. The 1:1:1 weight ratio of 22A: DPPC: POPC was selected for future examination. These 22A-sHDL particles had almost no impurities and a homogeneous size of 9.0 ± 0.1 nm. Many other studies verified that the size of natural human HDL ranges from 8.5 - 12.0 nm (28). To further confirm similarity of size for selected 22A-sHDL with endogenous HDL, purified human HDL was analyzed by GPC (Supplemental Figure S1). The retention time for endogenous human HDL was 7.35 min, demonstrating a size similarity to the selected 22A-sHDL.

3.2 Validation of LC-MS method for peptide quantification in serum

A new LC-MS method capable of accurate and sensitive detection of 22A and its main metabolite was developed. For this, we used a different apoA-I-mimetic peptide, 5A, as an internal standard. We have compared solid-state extraction of peptide from serum using Oasis® HLB extraction cartridges (Waters, Miford, MA) and organic solvent precipitation methods for sample preparation prior to LC-MS analysis. Product recovery using the solid-state extraction method was less than 30% (data was not shown). Using methanol to precipitate proteins, the peptide recovery was greater than 90% (29). The LC-MS analysis indicated a rapid decrease in 22A peak area in serum and the appearance of a terminal lysine-truncated metabolite (22A(-)Lys). The 22A(-)Lys metabolite was stable in plasma for up to 48 h. For the pharmacokinetic evaluation, a sum of serum concentrations of 22A and 22A (-)Lys was plotted as a function of time.

A limited validation was performed for serum extraction of peptide and LC-MS analysis. Linearity of the LC-MS analysis was observed for the peptide concentration range of 5 and 200 μg/mL, with $r^2 = 0.995$ (Supplemental Figure S2). The limit of quantification was determined to be 5 μg/mL. The extraction recovery of 22A ranged between 92 - 112 %. The accuracy of concentration determination for serum samples spiked with 22A at 6, 50, 160 μg/mL ranged from 7.8 to 12.0% of the target concentrations with precision (n = 6) ranging between 2.3% and 1.5%.

The inter-assay precision (n = 3) was between 3.8 - 4.3% (shown in Supplemental Table S1). Based on the analysis of percentage of 22A Lys (-) peptide in serum for the first four time points, metabolism appears to occur in a similar rapid manner for all four groups (as shown in Supplemental Figure S3).

3.3 Pharmacokinetic evaluation of apoA-I peptide

This experiment evaluated the dependence of apoA-I peptide's pharmacokinetics on its formulation and administration route. We found that following IV administration of either 22A solution of 22A-sHDL, peptide elimination followed first-order kinetics (Fig. 3A, B). As shown in Table 2, after IV dosing the clearance (*CL*) of 22A was more rapid when administered as free peptide than as 22A-sHDL particles (*CL* = 0.025 vs. 0.014 dL/h). Given the same volume of distribution between IV formulations (*Vd* = 0.13-14 dL), a similar increase was observed for the 22A elimination rate constant (K_{10} = 0.18 vs. 0.112 h^{-1}) with a concomitant decrease in the elimination half-life of 22A ($T_{1/2}$ = 3.81 vs. 6.27 h). As a result of the slower clearance, area under the 22A serum concentration-time curve (*AUC*) was 1.79-fold higher for 22A-sHDL than for the 22A peptide. This PK difference is significant and it is possibly due to peptide proteolysis *in vivo* or potentially different organs responsible for elimination of lipid-free peptide – kidney and sHDL particles – liver (30, 31). Following IP administration of 22A and 22A-sHDL, a first order absorption was observed from the injection site into the systemic circulation. The plasma peptide levels following IP administration were lower compared with IV administration and peaked at 4 h. The *AUC* of 22A, after IP dosing of 22A and 22A-sHDL, were only 52.0% and 54.1% of the IV administration, respectively. Since the vascular compartment is a target organ for most HDL therapeutics, dose adjustment appears to be critical since only about half of dose reaches the systemic circulation following IP administration.

No difference was observed when comparing the volume of distribution (*Vd*) of 22A after IV and IP administrations of 22A (i.e., 0.14 for IV and 0.16 dL [*Vd/F* × *F* or 0.30 × 0.52] for IP). Likewise, the clearance (*CL*) of 22A did not change between these two dosing routes (i.e., 0.025 for IV and 0.025 dL [*CL/F* × *F* or 0.048 × 0.52] for IP). As a result, the elimination rate constants (*K*) and half-lives ($T_{1/2}$) of 22A were very similar following IV and IP administrations. In contrast, the *Vd* of 22A was about 40% lower when administered as 22A-sHDL/IP (0.081 dL [*Vd/F* × *F* or 0.15 × 0.54]) as compared to 22A-sHDL/IV (0.13 dL). The reason for this difference is unclear but may be related to partial dissociation of 22A and phospholipid during absorption into systemic circulation following IP administration and peptide degradation/tissue binding during absorption. Since there was no difference in the *CL* of 22A after IV and IP treatments of 22A-sHDL (i.e., 0.014 for IV and 0.014 dL/h [*CL/F* × *F* or 0.026 × 0.54] for IP), the 22A elimination rate constant (*K*) was higher (0.17 vs. 0.11 h^{-1}) and the 22A half-life ($T_{1/2}$) lower (4.14 vs. 6.27 h) following IP administration as compared to IV dosing.

3.4 Phospholipid kinetics

Monitoring lipid plasma kinetics provides indirect information not only about the formation of HDL following administration of naked apoA-I peptide, but also about the *in vivo* stability of administered sHDL and elimination of its lipid component. Administration of apoA-I peptide in sHDL formulation at a dose of 75 mg/kg peptide dose corresponds to administration of 150 mg/kg of phospholipids (PL). The plasma levels of both endogenous and 22A-sHDL administered lipids were measured by choline oxidase assay. The elimination kinetics of total PL following 22A-sHDL injection are shown in Fig. 3C-F. After subtracting the pre-dose plasma PL levels, the pharmacokinetic parameters were determined and summarized in Table 3. The maximum PL level after IV injection of sHDL reached 483.0 mg/dL and constituted a 2.7-fold increase over the baseline PL level of 132.2 mg/dL (Fig. 3E). The AUC of PL after IV dosing of 22A-sHDL was 1559.6 mg*hr/dL. The AUC after IP administration of 22A-sHDL was 416.2

mg*hr/dL, indicating the bioavailability of lipids into the systemic circulation for IP injection was only 26.7%. Following IP administration of sHDL, the bioavailability of lipids is lower than that of 22A peptide (26.7% versus 54.1%), indicating some degree of dissociation of peptide from sHDL lipids during absorption. Although no exogenous PL was given in the case of peptide injection, it is believed that apoA-I mimetic peptides administered *in vivo* are capable of forming new HDL particles by lipid and cholesterol efflux via ATP-binding cassette transporter ABCA1 or by mobilizing phospholipid directly from cellular membranes (8, 32). Hence, the slight increase in plasma lipid levels is suggestive of de novo HDL formation. As shown in Fig. 3 C, D, a small increase in circulating lipids was observed for IV administration of 22A. In contrast, for IP administration of 22A, there was no obvious increase in plasma PL, likely due to tissue binding of peptide and decreased bioavailability to systemic circulation compared to IV dosing of peptide.

3.5 Cholesterol mobilization and esterification

To investigate the impact of lipidation and route of administration on apoA-I peptide ability to elicit pharmacological response, we examined the kinetics of plasma cholesterol biomarkers. Both free apoA-I peptide and sHDL infusions are capable of facilitating reverse cholesterol transport (RCT) by enhancing cholesterol efflux. Therefore, transient increases in plasma levels of cholesterol following treatment are expected. The kinetic changes in plasma total and unesterified cholesterol levels were measured directly by plate assays and the cholesterol ester levels were calculated (Fig. 4). Administration of 22A-sHDL by IV resulted in a rapid two-fold increase in total cholesterol (TC) within 0.5-1 h post-dose (Fig. 4A, B). The TC levels also increased slightly following IV administration of lipid-free 22A peptide ($p<0.05$ 0.25-2 h post-dose). In contrast, no statistically significant increase in TC was observed for administration of both lipid-free 22A and 22A-sHDL by IP route (Fig. 4A, B).

The mobilized cholesterol for 22A-sHDL infusions was predominantly unesterified or free cholesterol (Fig. 4 C, D). Normal pre-dose levels of rat plasma free cholesterol (FC) were approximately 11.7 mg/dL, and increased to 91.0 mg/dL within 1 h for IV dosing. The IP dosing of 22A-sHDL or IV dosing of lipid-free 22A also generated an increase in FC, but the effect was much smaller than that caused by IV injection of 22A-sHDL. There was no FC increase detected after IP peptide solution administration (Fig. 4 C, D). For 22A-sHDL IV administration, limited conversion of mobilized free cholesterol into cholesterol ester (CE) was observed (Fig. 4 E). It is possible that mobilized free cholesterol overwhelmed the esterification capacity of circulating LCAT, or that 22A-sHDL was not a good activator of rat lecithin cholesterol acyltransferase. Cholesterol seemed to be predominantly eliminated from plasma in its unesterified form following mobilization, and returned to the baseline levels 24 h post-dose. Hence, the pharmacological effect of apoA-I peptide was remarkably affected by the formulation and administration route, in which the IV dose of 22A-sHDL generated the strongest cholesterol transfer and mobilization efficacy.

3.6 Lipoprotein Distribution of Mobilized Cholesterol

In order investigate in greater detail the mechanism of cholesterol mobilization and elimination following apoA-I peptide or sHDL administrations, we determined the relative distribution of mobilized cholesterol in the HLD, LDL and VLDL fractions. Serum lipoproteins were separated by gel permeation chromatography and total cholesterol was detected following post-column enzymatic reaction (Fig. 5). Again, for the 22A-sHDL IV group, drastic but transient changes in lipoprotein profiles were observed over 24 h. Cholesterol was mobilized by injected HDL-sized particles, causing a rapid increase in particle size upon free cholesterol uptake. Since sHDL are prepared with a short, single-helical peptide, the size of the nanoparticle is not constrained by the length and structure of lipid bound full-length apoA-I, a major protein component of endogenous HDL. Therefore, we saw a rapid transition of cholesterol-carrying particles from HDL to LDL

size (15 min post-dose, with the maximum increase in cholesterol levels associated with LDL-sized particles detected by 2 h post-dose). While mobilization of FC was significant, the increase in levels of CE was disproportionally lower, indicating that cholesterol is likely to be taken up by the liver in its unesterified form (Figure 4D and F). At 2 h post-dose we also observed a significant increase in cholesterol levels in VLDL-sized lipoproteins. The VLDL-C increase could be due to saturation of liver receptors and enzymes that internalize, metabolize and secrete large amount of mobilized FC. However, the cholesterol changes were transient and lipoprotein-cholesterol distribution returned to a pre-dose profile 24 h post-dose. In contrast to 22A-sHDL IV group, only limited lipoprotein changes were observed for all other groups. A small transient increase in LDL-cholesterol level was observed for the 22A peptide group at 0.25 and 2 h post-dose, returning to baseline by 24 h post-dose. Due to limited cholesterol mobilization for all groups except for 22A-sHDL, it was difficult to assess differences in *in vivo* mechanisms of cholesterol efflux, mobilization, lipoprotein transfer and elimination for both lipid-fee peptide administrations and IP dosing of sHDL.

3.7 Plasma Remodeling

Potential differences in how apoA-I peptide or sHDL induce remodeling of endogenous lipoproteins were examined following *in vitro* incubation of both formulations with human serum. 22A and 22A-sHDL were added at 0, 0.15, 0.5, 1 and 3 mg/ml peptide concentrations, incubated for 30 min and separated by either 1-D native page electrophoresis (Fig. 6). The 1-D gels were visualized by western blot, staining for human apoA-I. The incubations were performed with a broad concentration range of 22A peptide, corresponding to *in vivo* concentration ranges of 0-1.5 mg/mL 22A, as measured by LC-MS. Compared to control serum (lane 1), all incubations showed reduction in the apoA-I content of α-HDL, seen by decreased stain intensity between 720 and 200 kDa. Along with this decrease, a 22A-peptide concentration dependent appearance of lipid-free or lipid-poor apoA-I protein was observed. The band of lipid-poor ApoA-I ran around

25-30 kDa and it had slightly higher intensity for 22A-serum incubations, but slightly larger size for 22A-sHDL-serum incubation. Hence, both naked and lipid-bound 22A were capable of associating with endogenous HDL and displacing endogenous apoA-I on HDL particles. Lipoprotein remodeling and release of lipid free apoA-I could potentially be responsible for the therapeutic effect, independent of cholesterol mobilization and RCT.

3.8 Pharmacokinetics and pharmacodynamics correlation

Based on experimental pharmacokinetic (PK) and free cholesterol mobilization pharmacodynamic (PD) data, the indirect response PK-PD models were developed for 22A and phospholipids (Figure 1). The parameters obtained from PK-PD modeling allow for the prediction of timing and magnitude of FC increase, such that the dosing regimens can be further optimized. The best fit for the PK data was obtained using a one-compartment disposition model, with lowest Akaike Information Criterion (AIC) values for both IV and IP injections without lag time. PD parameters obtained from 22A-FC or phospholipids-FC PK-PD models are listed in Table 4. For IP injection of the 22A group, the model failed to fit the data because FC mobilization was limited for this group.

In all four groups, a plot of the relationship between 22A serum concentration and FC levels showed an anticlockwise hysteresis, indicating a significant delay in peak levels of free cholesterol relative to the C_{max} of 22A or phospholipids (Fig. 7). This relationship was described by an indirect response model in which serum concentrations of 22A or PL had a stimulatory effect on the production of FC. Under normal physiological condition without HDL injection the endogenous free cholesterol level change can be described by a basic turnover model, which includes a zero-order turnover or synthesis rate constant (k_{in}) and a first-order rate constant for cholesterol elimination (k_{out}). 22A or 22A-sHDL worked as stimulatory factors having an effect on production of the response (Fig. 1). Among all stimulation functions, the infinite stimulation model fits the data best, giving the lowest sum of squared residual value. The parameters k_{in} and

k_{out} are independent of drug concentration, thus estimated values for all three groups were similar. The free cholesterol baseline level R_0, which is assumed to be constant, can be calculated by $R_0 = k_{in}/k_{out}$ for the three modeled groups. Similar baseline values were observed to be approximately 12 mg/dL, meeting the values detected for pre-dose.

There was no significant difference between the sigmoidicity factor gamma (γ), except in the case of the 22A-PD model for the 22A-sHDL IP group, whose value was much lower than IV group. The EC_{50} represents the plasma concentration needed to achieve a 50% of maximum stimulation achieved at the effect site of a dosed agent. From Table 4, 22A peptide had a significantly lower EC_{50} value after IV dosing of 22A-sHDL than after IV dosing of free peptide (53.8 mg/dL versus 142.8 mg/dL), indicating that the sHDL formulation had a more potent effect on cholesterol efflux than did the free peptide. There was no significant difference between the 22A-sHDL IV and IP groups. Combining EC_{50} and γ values, lipidation of 22A increases the potency of peptide whereas altering the administration route can increase the sensitivity of cholesterol efflux towards any 22A concentration change at the effect site. However, the smaller value of phospholipids EC_{50} value for phospholipids in the 22A-sHDL IV group compared to IP groups (27.1 mg/dL versus 74.0 mg/dL) showed that the phospholipids in sHDL triggered higher cholesterol efflux after IV injection compared to IP injection at the same dose, which may result from sHDL particle dis-assembly during the absorption process (Table 5).

The log-likelihood value reflects the quality of the fitted model. In the 22A-sHDL IP group, the phospholipid-FC PK/PD model appears to provide a better fit for the data compared to the 22A-FC PK/PD models, as highlighted by the larger LogLik values (Tables 4 and Table 5). This better fit underscores the notion that FC mobilization is likely elicited by the presence of cholesterol-free lipid bilayers of sHDL in the plasma and to a lesser degree by peptide-mediated cholesterol efflux.

4. Discussion

We found that both the physical state of the apoA-I peptide (i.e. naked or lipid-bound sHDL) and the route of administration (IV versus IP) profoundly affected its pharmacokinetics and the mechanism of eliciting pharmacological response. Only lipidated 22A-sHDL administered by IV resulted in rapid and massive mobilization of free cholesterol. Additionally, only a partial conversion of FC to CE was observed, and all mobilized cholesterol was subsequently eliminated within 24 h. The difference in plasma-mobilized cholesterol levels did not directly correlate with differences in the pharmacokinetics of apoA-I peptide administered in a lipid-free form or in the bioavailability of apoA-I peptide to systemic circulation following IP dosing. The half-life of peptide administered in lipid-free form was only 0.61-fold shorter relative to 22A-sHDL. However, 1-2 h post-dose the maximum levels of mobilized FC reached 22 mg/dL for 22A and 91 mg/dL for 22A-sHDL (Fig. 4 C, D, Table 2), constituting a 1.3 and 5.3 increase from pre-dose level, respectively. This significant difference in the magnitude of plasma cholesterol mobilization indicated a potential mechanistic difference in how cholesterol efflux is elicited for lipid-free peptide and sHDL *in vivo*. The rapid cholesterol mobilization following IV administration of sHDL was likely caused in part by a physical partitioning of FC from cellular membranes to cholesterol-free lipid bilayers of sHDL. For administration of lipid-free 22A peptide, cholesterol mobilization possibly occurs in a receptor-mediated manner following interaction with peptide or *de novo* formed HDL following of plasma remodeling of lipoprotein by 22A peptide. Extensive mobilization of FC in serum led to rapid conversion of the injected sHDL particles to LDL-sized, cholesterol-loaded particles, causing a spike in LDL-C levels between 2-8 hours post-dose. These transient increases in LDL-C and triglyceride levels have been observed previously for both free ApoA-I and HDL infusions, and has been attributed to saturating the liver's capacity to excrete free cholesterol and inhibiting hepatic and lipoprotein lipases (33). While the changes in lipoproteins appeared to be very dramatic following 22A-

sHDL IV infusion, they were also transient, as all lipoprotein levels returned to baseline 24-hours post-dose. Similar transient changes in lipoproteins have been observed in clinical settings for infusions of other HDL products, such as CER-001 (34) and ETC-216 (35).

When either lipid-free or lipidated peptide was mixed with serum, each was capable of remodeling of endogenous lipoproteins, leading to the appearance of a lipid-poor apoA-I fraction. The appearance of lipid-poor apoA-I indicates that, upon administration, 22A peptide binds to endogenous HDL particles and causes endogenous apoA-I displacement from HDL. It is unclear how this phenomenon impacts the anti-atherosclerotic activity of apoA-I mimetic peptide as well as how the sequences of various peptides influence endogenous lipoprotein binding. The PK-PD modeling that correlated 22A with an increase in FC, a plasma biomarker of cholesterol efflux, revealed EC_{50} values to be much lower for 22A-sHDL-IV compared with lipid-free-22A-IV (Table 4).

The initial decision to use reconstituted HDL particles rather than lipid-free apoA-I in clinical development occurred in the 1990s following the first clinical evaluation by Miller *et al* (3, 15). In these studies, prolonged IV infusion and bolus administration of lipid-free apoA-I up to 50 mg/kg dose failed to increase plasma levels of HDL-C. Instead, transient increases in LDL particles were noted and attributed to inhibition of lipoprotein and hepatic lipases. In contrast, infusions of reconstituted HDL particles at 25 and 40 mg/kg of apoA-I resulted in transient increases in HDL unesterified cholesterol levels, followed by cholesterol esterification and elimination. Since these first clinical trials, the elevation of HDL-C levels has become a primary biomarker of sHDL's pharmacological effect. The clinical dose selection and preclinical optimization for many follow-on HDL products (ETC-642, CER-001) were performed based on the HDL-C increase as biomarker (2, 5). However, it is becoming clear that there are mechanistic differences in how sHDL and free apoA-I elicit cholesterol efflux. Lipid-free apoA-I interacts with ABCA-1 receptors to efflux, forms *de novo* HDL and remodel existing lipoproteins. In contrast, the cholesterol-free lipid bilayers of sHDL particles are strong acceptors of cholesterol

from ABCG1, SR-BI, and via passive efflux from cellular membranes. Indeed, recent studies have shown that SR-BI receptors are largely responsible for free cholesterol elevation following rHDL infusion, and that phospholipids, not ApoA-I, dictate FC efflux (36, 37). Because of these factors, CSL-112 pharmacological efficacy in early clinical trials was monitored by increases in ABCA1 cholesterol efflux capacity of patient plasma following drug administration (38).

Several studies have directly compared the anti-inflammatory effects of apoA-I and HDL administered by IV infusion in animal models of arthritis (11) and a carotid peri-arterial collar model (12). When lipid-free apoA-I and reconstituted HDL were administered at a low dose of 8 mg/kg, they exhibited similar measurable anti-inflammatory activity. This indicates that some of protective mechanisms of apoA-I and sHDL infusions could not be characterized simply by monitoring cholesterol mobilization, and additional biomarkers are needed to establish the PK-PD relationship.

Direct comparisons of the anti-atherosclerotic potency of IP injections of 30 mg/kg of either ATI-5261 peptide or reconstituted HDL were performed in a high-fat diet fed ApoE-/- mouse model of atherosclerosis (39). While no increase in plasma cholesterol levels was detected, sHDL injections showed slightly better atheroma reduction, however the difference was not statistically significant. In our study, IP administrations resulted in only limited plasma cholesterol mobilization, with slightly higher mobilization for sHDL infusions compared to those using lipid-free peptide. Following IP dosing 52% of lipid-free apoA-I peptide, 54% of lipidated apoA-I peptide and 27% of sHDL phospholipids reached the systemic circulation. In addition, the values for absorption (K_{01}) and elimination (K_{10}) constants differed for PL and 22A following IP administration of 22A-sHDL (Tables 2 and 3), indicating that some of 22A-sHDL was dissociated prior to absorption. Peptide tissue-binding, proteolysis and disassembly of 22A-sHDL particles are potential reasons for the reduced and different bioavailabilities. Peptide tissue-binding and proteolysis depend on the primary sequence of peptide and, thus, differ for various

peptides and full-length apoA-I. Stability of sHDL *in vivo* and extent of endogenous HDL remodeling depend on the lipid binding affinity of amphipathic helixes toward lipid used in sHDL formulation, endogenous lipoproteins and plasma lipid membrane as well as the peptide's tendency to self-associate (4, 40). Furthermore, lipid formulation of sHDL (peptide-lipid ratio, lipid type and sHDL particle size) affects particle stability, cholesterol affinity and interaction with LCAT (41). Thus, *in vivo* behavior of apoA-I peptide and sHDL formulation could be distinctly different for various peptide sequences and lipid formulations.

The magnitude of cholesterol mobilization and pharmacokinetic parameters depend on the dose of administered apoA-I peptide. The dose used in this study, 75 mg/kg, was selected to assure the detection of peptide in plasma following IP administration. The selected dose is slightly higher than doses used in animal pharmacology studies for apoA-I and HDL, which range between 1 and 50 mg/kg (42, 43). However, in phase I clinical dosing the infusions were given up to 45 mg/kg for CER-001, 135 mg/kg for CSL-112 and 50 mg/kg for lipid free apoA-I (2-4). Hence, 75 mg/kg was a reasonable dose for the current study. In addition, our study was conducted in healthy rats to allow for the multiple blood draws required to determine for PK and PD parameters. However, the cholesterol pool mobilized in healthy rats is likely to be different from that present in human atheromas and, thus it would be beneficial to evaluate how apoA-I lipidation affects cholesterol mobilization in hyperlipidemic disease models.

The results of this study emphasize the criticality of considerations for formulation, route of administration, and dose used in pharmacological studies of apoA-I peptide and sHDL particles. Historic drug development considerations for the selection of HDL dose and formulation were based on measurements of plasma cholesterol level increase, which were primarily observed upon IV administration of sHDL particles. Yet, the increase in plasma cholesterol primarily depends on sHDL lipid composition and particle stability *in vivo*, and is seen upon administration of relatively high doses of sHDL. Thus, endogenous lipoporotein remodeling, anti-inflammatory effects and apoA-I protein mediated ABCA-1 efflux that are exhibited at lower doses are often

underemphasized. Consequently, a mechanistic understanding of which therapeutics effects of sHDL are mediated by lipoprotein particles and which are mediated by their apoA-I component, as well as correlating elicited pharmacologic effect *in vivo* with the actual systemic concentrations, AUC and pharmacokinetic parameters for administered apoA-I peptide, will significantly improve clarity around the development of HDL mimetics. Identification of *in vivo* biomarkers indicative of HDL mimetic potency in addition to HDL-C plasma increase and rapid assessment of *in vivo* of PK and biomarker response for novel apoA-I mimetic peptides could improve their development outcomes, as extensive *in vitro* optimization does not account for peptide proteolysis and excessive tissue binding *in vivo*.

5. Acknowledgements

The authors wish to acknowledge Mass Spectrometry Core, University of Michigan Department of Chemistry. This research was funded in part by AHA 13SDG17230049 (AS), AHA 16POST27760002 (WY), Michigan College of Pharmacy Upjohn Award, NIH R01 GM113832 and R21 NS091555. Emily E. Morin was partially supported by a fellowship from the Cellular Biotechnology Training Program (T32 GM008353) and Translational Cardiovscular Research and Entrepreneurship Training Grant (T32 HL125242). Lindsey Drake was partially supported by a fellowship from the Pharmacological Sciences Training Program (T32 GM07767). Sara Deschaine was supported by a fellowship from Interdisciplinary REU Program in the Structure and Function of Proteins (NSF DBI #1263079).

References

1. Smith, J. D. 2010. Apolipoprotein AI and its mimetics for the treatment of atherosclerosis. *Curr. Opin. Investig. Drug* **11**: 989.

2. van Capelleveen, J. C., H. B. Brewer, J. J. Kastelein, and G. K. Hovingh. 2014. Novel therapies focused on the high-density lipoprotein particle. *Circ. Res.* **114**: 193-204.

3. Nanjee, M., J. Crouse, J. King, R. Hovorka, S. Rees, E. Carson, J.-J. Morgenthaler, P. Lerch, and N. Miller. 1996. Effects of intravenous infusion of lipid-free apo AI in humans. *Arterioscler. Thromb. Vasc. Biol.* **16**: 1203-1214.

4. Kuai, R., D. Li, Y. E. Chen, J. J. Moon, and A. Schwendeman. 2016. High-density lipoproteins: nature's multifunctional nanoparticles. *ACS Nano.* **10**: 3015-3041.

5. Nissen, S. E., T. Tsunoda, E. M. Tuzcu, P. Schoenhagen, C. J. Cooper, M. Yasin, G. M. Eaton, M. A. Lauer, W. S. Sheldon, and C. L. Grines. 2003. Effect of recombinant ApoA-I Milano on coronary atherosclerosis in patients with acute coronary syndromes: a randomized controlled trial. *Jama.* **290**: 2292-2300.

6. Osei-Hwedieh, D. O., M. Amar, D. Sviridov, and A. T. Remaley. 2011. Apolipoprotein mimetic peptides: Mechanisms of action as anti-atherogenic agents. *Pharmacol. Ther.* **130**: 83-91.

7. Favari, E., L. Calabresi, M. P. Adorni, W. Jessup, S. Simonelli, G. Franceschini, and F. Bernini. 2009. Small discoidal pre-β1 HDL particles are efficient acceptors of cell cholesterol via ABCA1 and ABCG1. *Biochemistry.* **48**: 11067-11074.

8. Duong, P. T., G. L. Weibel, S. Lund-Katz, G. H. Rothblat, and M. C. Phillips. 2008. Characterization and properties of preβ-HDL particles formed by ABCA1-mediated cellular lipid efflux to apoA-I. *J. Lipid Res.* **49**: 1006-1014.

9. Kee, P., K.-A. Rye, J. L. Taylor, P. H. R. Barrett, and P. J. Barter. 2002. Metabolism of apoA-I as lipid-free protein or as component of discoidal and spherical reconstituted HDLs: studies in wild-type and hepatic lipase transgenic rabbits. *Arterioscler. Thromb. Vasc. Biol.* **22**: 1912-1917.

10. Patel, S., B. A. Di Bartolo, S. Nakhla, A. K. Heather, T. W. Mitchell, W. Jessup, D. S. Celermajer, P. J. Barter, and K.-A. Rye. 2010. Anti-inflammatory effects of apolipoprotein AI in the rabbit. *Atherosclerosis.* **212**: 392-397.

11. Wu, B. J., K. L. Ong, S. Shrestha, K. Chen, F. Tabet, P. J. Barter, and K.-A. Rye. 2014. Inhibition of arthritis in the Lewis rat by apolipoprotein AI and reconstituted high-density lipoproteins. *Arterioscler. Thromb. Vasc. Biol.* **34**: 543-551.

12. Nicholls, S. J., G. J. Dusting, B. Cutri, S. Bao, G. R. Drummond, K.-A. Rye, and P. J. Barter. 2005. Reconstituted high-density lipoproteins inhibit the acute pro-oxidant and proinflammatory vascular changes induced by a periarterial collar in normocholesterolemic rabbits. *Circulation.* **111**: 1543-1550.

13. Peterson, S. J., D. Husney, A. L. Kruger, R. Olszanecki, F. Ricci, L. F. Rodella, A. Stacchiotti, R. Rezzani, J. A. McClung, and W. S. Aronow. 2007. Long-term treatment with the apolipoprotein A1 mimetic peptide increases antioxidants and vascular repair in type I diabetic rats. *J. Pharm. Exp. Ther.* **322**: 514-520.

14. Shah, P. K., J. Yano, O. Reyes, K.-Y. Chyu, S. Kaul, C. L. Bisgaier, S. Drake, and B. Cercek. 2001. High-dose recombinant apolipoprotein a-imilano mobilizes tissue cholesterol and rapidly reduces plaque lipid and macrophage content in apolipoprotein e–deficient mice potential implications for acute plaque stabilization. *Circulation.* **103**: 3047-3050.

15. Nanjee, M., J. Doran, P. Lerch, and N. Miller. 1999. Acute effects of intravenous infusion of ApoA1/phosphatidylcholine discs on plasma lipoproteins in humans. *Arterioscler. Thromb. Vasc. Biol.* **19**: 979-989.

16. Remaley, A. T., M. Amar, and D. Sviridov. 2008. HDL-replacement therapy: mechanism of action, types of agents and potential clinical indications. *Expert Rev. Cardiovasc. Ther.* **6**: 1203-1215.

17. Sharifov, O. F., X. Xu, A. Gaggar, W. E. Grizzle, V. K. Mishra, J. Honavar, S. H. Litovsky, M. N. Palgunachari, C. R. White, and G. Anantharamaiah. 2013. Anti-inflammatory mechanisms

of apolipoprotein AI mimetic peptide in acute respiratory distress syndrome secondary to sepsis. *PLoS One* **8**: e64486.

18. Meibohm, B., and H. Derendorf. 2002. Pharmacokinetic/pharmacodynamic studies in drug product development. *J. Pharm. Sci.* **91**: 18-31.

19. Olsen, C. K., L. T. Brennum, and M. Kreilgaard. 2008. Using pharmacokinetic-pharmacodynamic modelling as a tool for prediction of therapeutic effective plasma levels of antipsychotics. *Eur. J. Pharmacol.* **584**: 318-327.

20. Li, D., S. Gordon, A. Schwendeman, and A. T. Remaley. 2015. Apolipoprotein mimetic peptides for stimulating cholesterol efflux. *In* Apolipoprotein mimetics in the management of human disease. Springer. 29-42.

21. Miles, J. 2004. Single-dose tolerability, pharmacokinetics, and cholesterol mobilization in HDL-C fraction following intravenous administration of ETC-642, a 22-mer ApoA-I analogue and phospholipids complex, in atherosclerosis patients. *Arterioscler. Thromb. Vasc. Biol.* **24**: E19.

22. Dayneka, N. L., V. Garg, and W. J. Jusko. 1993. Comparison of four basic models of indirect pharmacodynamic responses. *J. Pharmacokinet. Biopharm.* **21**: 457-478.

23. Garber, D. W., K. R. Kulkarni, and G. M. Anantharamaiah. 2000. A sensitive and convenient method for lipoprotein profile analysis of individual mouse plasma samples. *J. Lipid Res.* **41**: 1020-1026.

24. Freeman, L. A. 2013. Native–native 2D gel electrophoresis for HDL subpopulation analysis. *Lipoproteins and Cardiovascular Disease: Methods and Protocols*: 353-367.

25. Stoekenbroek, R., E. Stroes, and G. Hovingh. 2015. ApoA-I mimetics. *In* High Density Lipoproteins. Springer. 631-648.

26. Subbaiah, P., and M. Liu. 1993. Role of sphingomyelin in the regulation of cholesterol esterification in the plasma lipoproteins. Inhibition of lecithin-cholesterol acyltransferase reaction. *J. Biol. Chem.* **268**: 20156-20163.

27. Dasseux, J.-L., A. S. Schwendeman, and L. Zhu. 2015. Apolipoprotein ai mimics. *In*. Google Patents. EP2396017 A2396014.

28. Anderson, D. W., A. V. Nichols, T. M. Forte, and F. T. Lindgren. 1977. Particle distribution of human serum high density lipoproteins. *Biochim. Biophys. Acta* **493**: 55-68.

29. Tamvakopoulos, C. 2007. Mass spectrometry for the quantification of bioactive peptides in biological fluids. *Mass Spectrom. Rev.* **26**: 389-402.

30. Spady, D. K., L. A. Woollett, R. S. Meidell, and H. H. Hobbs. 1998. Kinetic characteristics and regulation of HDL cholesteryl ester and apolipoprotein transport in the apoA-I-/-mouse. *J. Lipid Res.* **39**: 1483-1492.

31. Horowitz, B., I. Goldberg, J. Merab, T. Vanni, R. Ramakrishnan, and H. Ginsberg. 1993. Increased plasma and renal clearance of an exchangeable pool of apolipoprotein AI in subjects with low levels of high density lipoprotein cholesterol. *J. Clin. Invest.* **91**: 1743.

32. Lu, S.-C., L. Atangan, K. W. Kim, M. M. Chen, R. Komorowski, C. Chu, J. Han, S. Hu, W. Gu, and M. Véniant. 2012. An apoA-I mimetic peptibody generates HDL-like particles and increases alpha-1 HDL subfraction in mice. *J. Lipid Res.* **53**: 643-652.

33. Dasseux, J.-L., and R. Ackermann. 2015. Lipoprotein complexes and manufacturing and uses thereof. *In*. Google Patents. US9187551 B9187552.

34. Kootte, R. S., L. P. Smits, F. M. van der Valk, J.-L. Dasseux, C. H. Keyserling, R. Barbaras, J. F. Paolini, R. D. Santos, T. H. van Dijk, and G. M. Dallinga-van Thie. 2015. Effect of open-label infusion of an apoA-I-containing particle (CER-001) on RCT and artery wall thickness in patients with FHA. *J. Lipid Res.* **56**: 703-712.

35. Bisgaier, C. L., R. Ackermann, T. Rea, W. V. Rodrigueza, and D. Hartman. 2016. ApoA-IMilano phospholipid complex (ETC-216) infusion in human volunteers. Insights into the phenotypic characteristics of ApoA-IMilano carriers. *Pharmacol. Res.* **111**: 86-99.

36. Cuchel, M., S. Lund-Katz, M. de la Llera-Moya, J. S. Millar, D. Chang, I. Fuki, G. H. Rothblat, M. C. Phillips, and D. J. Rader. 2010. Pathways by which reconstituted high-density

lipoprotein mobilizes free cholesterol from whole body and from macrophages. *Arterioscler. Thromb. Vasc. Biol.* **30**: 526-532.

37. Herzog, E., I. Pragst, M. Waelchli, A. Gille, S. Schenk, J. Mueller-Cohrs, S. Diditchenko, P. Zanoni, M. Cuchel, and A. Seubert. 2016. Reconstituted high-density lipoprotein can elevate plasma alanine aminotransferase by transient depletion of hepatic cholesterol: role of the phospholipid component. *J. Appl. Toxicol.* **36**: 1038-1047.

38. Gille, A., R. Easton, D. D'Andrea, S. D. Wright, and C. L. Shear. 2014. CSL112 enhances biomarkers of reverse cholesterol transport after single and multiple infusions in healthy subjects. *Arterioscler. Thromb. Vasc. Biol.* **34**: 2106-2114.

39. Bielicki, J. K., H. Zhang, Y. Cortez, Y. Zheng, V. Narayanaswami, A. Patel, J. Johansson, and S. Azhar. 2010. A new HDL mimetic peptide that stimulates cellular cholesterol efflux with high efficiency greatly reduces atherosclerosis in mice. *J. Lipid Res.* **51**: 1496-1503.

40. Yancey, P. G., J. K. Bielicki, W. J. Johnson, S. Lund-Katz, M. N. Palgunachari, G. Anantharamaiah, J. P. Segrest, M. C. Phillips, and G. H. Rothblat. 1995. Efflux of cellular cholesterol and phospholipid to lipid-free apolipoproteins and class A amphipathic peptides. *Biochemistry.* **34**: 7955-7965.

41. Schwendeman, A., D. O. Sviridov, W. M. Yuan, Y. H. Guo, E. E. Morin, Y. Yuan, J. Stonik, L. Freeman, A. Ossoli, S. Thacker, S. Killion, M. Pryor, Y. E. Chen, S. Turner, and A. T. Remaley. 2015. The effect of phospholipid composition of reconstituted HDL on its cholesterol efflux and anti-inflammatory properties. *J. Lipid Res.* **56**: 1727-1737.

42. Di Bartolo, B. A., S. J. Nicholls, S. Bao, K.-A. Rye, A. K. Heather, P. J. Barter, and C. Bursill. 2011. The apolipoprotein AI mimetic peptide ETC-642 exhibits anti-inflammatory properties that are comparable to high density lipoproteins. *Atherosclerosis.* **217**: 395-400.

43. Iwata, A., S.-i. Miura, B. Zhang, S. Imaizumi, Y. Uehara, M. Shiomi, and K. Saku. 2011. Antiatherogenic effects of newly developed apolipoprotein AI mimetic peptide/phospholipid

complexes against aortic plaque burden in Watanabe-heritable hyperlipidemic rabbits. *Atherosclerosis.* **218**: 300-307.

Table 1. The characterization summary of different 22A-sHDL particles

sHDL formulations (wt/wt/wt ratio)	Retention time (min)	Particle size (nm)	Polydispersity index
DPPC:POPC:22A (2:2:1)	7.02	12.5 ± 0.1	0.29 ± 0.07
DPPC:POPC:22A (1.5:1.5:1)	7.32	10.5 ± 0.1	0.17 ± 0.06
DPPC:POPC:22A (1:1:1)	7.80	9.0 ± 0.1	0.16 ± 0.03
DPPC:POPC:22A (0.5: 0.5:1)	8.83	7.4 ± 0.1	0.23 ± 0.04
DPPC:POPC:22A (0.25:0.25:1)	9.16	5.5 ± 0.1	0.56 ± 0.09

Table 2. Pharmacokinetic parameters (% CV) of 22A peptide after 75 mg/kg doses of 22A by four different treatments.

Parameters	Groups			
	22A/IV	22A/IP	22A-sHDL/IV	22A-sHDL/IP
T_{max} (h)	–	4.27 (15.3)	–	4.04 (21.5)
C_{max} (mg/dL)	152.16 (5.0) ^{ns}	34.83 (14.0) ****	165.23 (7.6)	68.87 (19.9) ****
AUC (mg*h/dL)	836.3 (7.8) ***	434.5 (17.3) ****	1495.5(13.9)	809.4 (24.6) ***
K_{01} (h^{-1})	–	0.33 (34.3)	–	0.35 (47.7)
K_{10} (h^{-1})	0.18 (9.6) **	0.16 (10.9) *	0.11 (16.6)	0.17 (14.4) *
$T_{1/2}$ (h)	3.81 (9.6) ***	4.43 (10.9) **	6.27 (16.6)	4.14 (14.4) **
CL (dL/h)	0.025 (7.8) ^{ns}	0.048 (17.4) ****	0.014 (13.9)	0.026 (24.6) *
V_d (dL)	0.14 (5.0) ^{ns}	0.30 (26.1) **	0.13 (7.6)	0.15 (36.16) ^{ns}
AIC	15.48	12.35	23.36	7.00

Mean ± S.D. (n = 3), *p<0.05, **p<0.01, ***p<0.001, ****p<0.0001, ns: no significant difference compared with 22A-sHDL/IV treatment. T_{max}: Time at which the C_{max} is observed; C_{max}: the maximum plasma concentration of 22A; ***AUC***: the area under the curve in plot of concentration of 22A against time; k_{01}: the first-order absorption rate constant; k_{10}: the first order elimination rate constant; $T_{1/2}$: the half-life of elimination; ***CL***: apparent total clearance for 22A (*CL* for IV and *CL*/*F* for IP, where *F* is bioavailability); V_d: apparent volume of distribution for 22A (*Vd* for IV and *Vd*/*F* for IP, where *F* is bioavailability); ***AIC:*** Akaike Information Criterion.

Table 3. Pharmacokinetic parameters (% CV) of phospholipids after 150 mg/kg doses of phospholipids by two different treatments

Parameters	Groups	
	22A-sHDL/IV	22A-sHDL/IP
T_{max} (h)	–	2.33 (14.6)
C_{max} (mg/dL)	420.9 (2.9)	58.3 (10.1)
AUC (mg*h/dL)	1559.6 (3.9)	416.2 (14.2) ****
K_{01} (h^{-1})	–	0.67 (46.9)
K_{10} (h^{-1})	0.27 (4.9)	0.25 (40.2)
$T_{1/2}$ (h)	2.57 (4.9)	2.74 (40.2) ns
CL (dL/h)	0.027 (3.9)	0.10 (14.2) **
V_d (dL)	0.10 (2.9)	0.40 (35.1) *
AIC	13.51	19.34

Mean ± S.D. (n = 3), *p<0.05, **p<0.01, ****p<0.0001, ns: no significant difference compared with 22A-sHDL/IV treatment. T_{max}: Time at which the C_{max} is observed; C_{max}: the maximum plasma concentration of phospholipid; *AUC*: the area under the curve in plot of concentration of phospholipid against time; k_{01}: the first-order absorption rate constant; k_{10}: the first order elimination rate constant; $T_{1/2}$: the half-life of elimination; *CL*: apparent clearance for phospholipid (*CL* for IV and *CL*/*F* for IP, where *F* is bioavailability); V_d: apparent volume of distribution for phospholipid (*Vd* for IV and *Vd*/*F* for IP, where *F* is bioavailability); ***AIC:*** Akaike Information Criterion.

Table 4. Estimated pharmacodynamic parameters (with % CV of the estimate) for 22A peptide.

Parameters	Groups			
	22A/IV	**22A/IP**	**22A-sHDL/IV**	**22A-sHDL/IP**
k_{in} **(mg/(dL*h))**	30.38 (53.7)	–	30.48 (18.3)	30.60 (70.4)
k_{out} **(h^{-1})**	2.65 (61.6)	–	2.61 (10.5)	3.46 (60.1)
EC_{50} **(mg /dL)**	142.81 (8.6) ***	–	53.77 (21.2)	47.63 (247.8) ns
gamma	2.08 (71.9) ns	–	1.92 (10.6)	0.36 (90.6) ***
LogLik	-9.96	–	-15.97	-11.94

Mean ± S.D. (n = 3), ***p<0.001, ns: no significant difference versus 22A-sHDL/IV group. k_{in}: the zero-order constant for production of response; k_{out}: the first-order constant for loss of the response; EC_{50}: the plasma concentration needed to achieve a 50% of maximum stimulation achieved at the effect site of a dosed agent; ***gamma***: steepness of the sigmoidal curve. **LogLik**: Log-likelihood of best-fitted model.

Table 5. Estimated pharmacodynamic parameters (with % CV of the estimate) for phospholipids.

Parameters	Groups	
	22A-sHDL/IV	22A-sHDL/IP
k_{in} (mg/(dL*hr))	30.48 (18.2)	22.26 (27.2)
k_{out} (hr^{-1})	2.61 (10.5)	1.85 (27.3)
EC_{50} (mg /dL)	27.11 (51.6)	74.02 (9.93) *
gamma	0.78 (10.6)	1.25 (25.2) ns
LogLik	-15.97	-7.34

Mean ± S.D. (n = 3), *p<0.05, ns: no significant difference versus 22A-sHDL/IV group. k_{in}: the zero-order constant for production of response; k_{out}: the first-order constant for loss of the response; EC_{50}: the plasma concentration needed to achieve a 50% of maximum stimulation achieved at the effect site of a dosed agent; ***gamma***: steepness of the sigmoidal curve. **LogLik**: Log-likelihood of best-fitted model.

Figure 1:

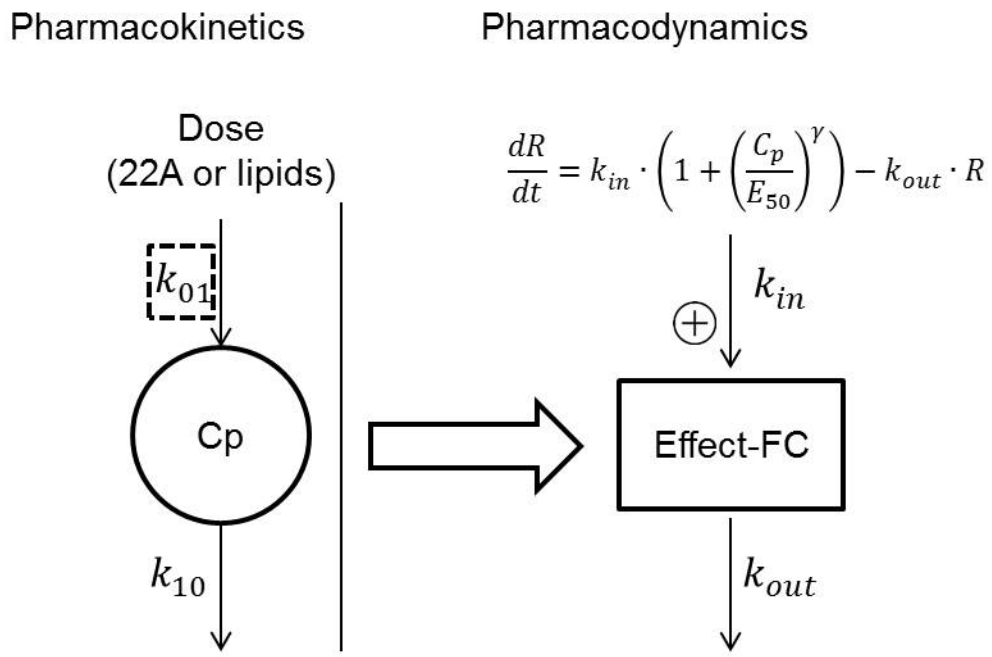

Figure 1. Scheme of the pharmacokinetic-pharmacodynamic (PK-PD) model based on a one-compartment PK model. k_{01}: the first-order absorption rate constant for IP groups only; k_{10}: the first order elimination rate constant; k_{in}: the zero-order constant for production of response; k_{out}: the first-order constant for loss of the response; EC_{50}: the serum concentration needed to achieve a 50% of maximum stimulation achieved at the effect site of a dosed agent; γ: steepness of the sigmoidal curve.

Figure 2:

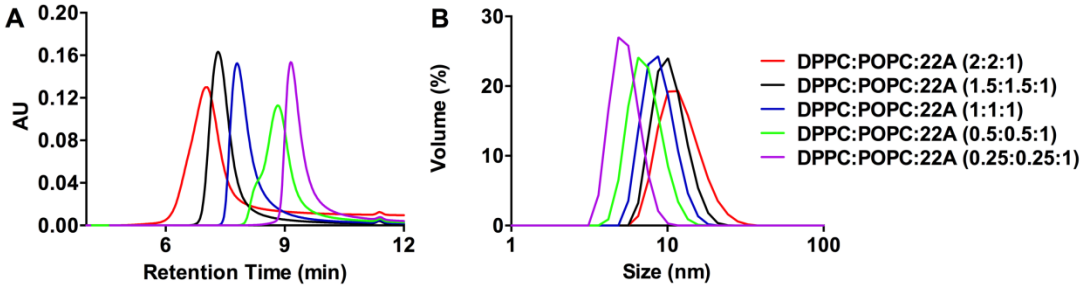

Figure 2. Characterization of 22A reconstituted sHDL particles. Gel permeation chromatography (A), dynamic light scattering (B).

Figure 3:

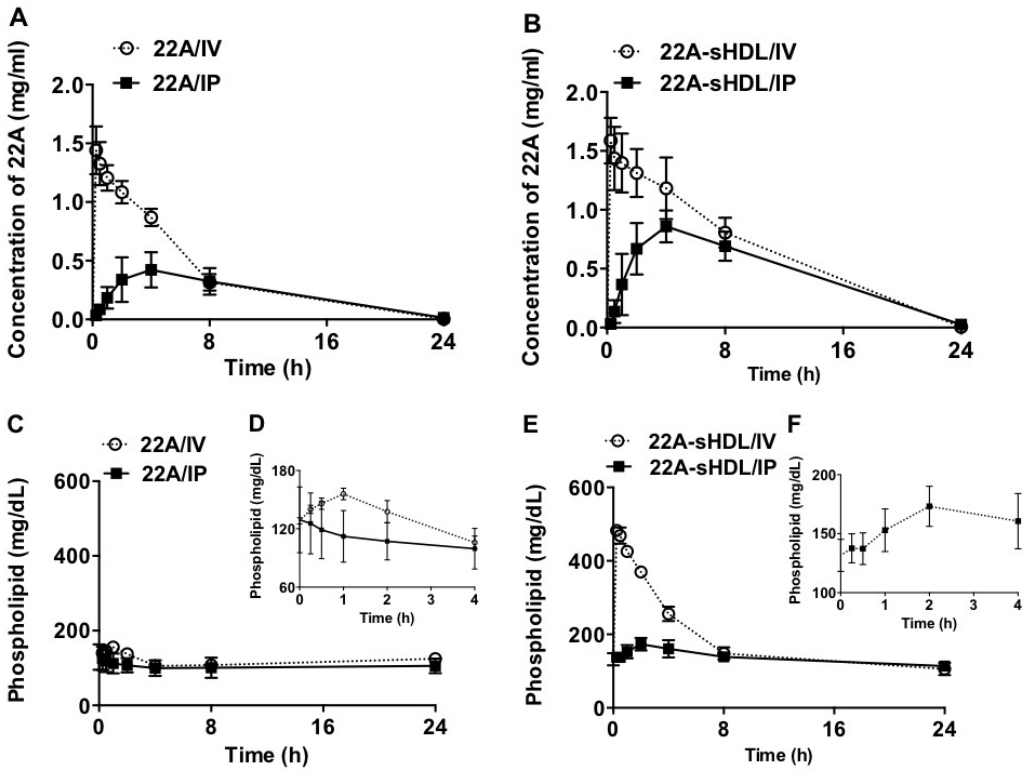

Figure 3. Pharmacokinetics of 22A peptide after administration of lipid-free 22A peptide (panel A) or 22A-sHDL (panel B). The kinetics of phospholipid mobilization and elimination following administration of lipid-free 22A peptide (panel C and insert D) or 22A-sHDL (panel E and insert F). Sprague-Dawley rats received 75 mg/kg of 22A or 22A-sHDL by either IV or IP injection. For 22A-sHDL a dose of 75 mg/kg of peptide corresponded to a 150 mg/kg dose of phospholipids. Serum peptide concentrations were determined by LC-MS and total choline containing phospholipids was measured by a commercial choline oxidase assay.

Figure 4:

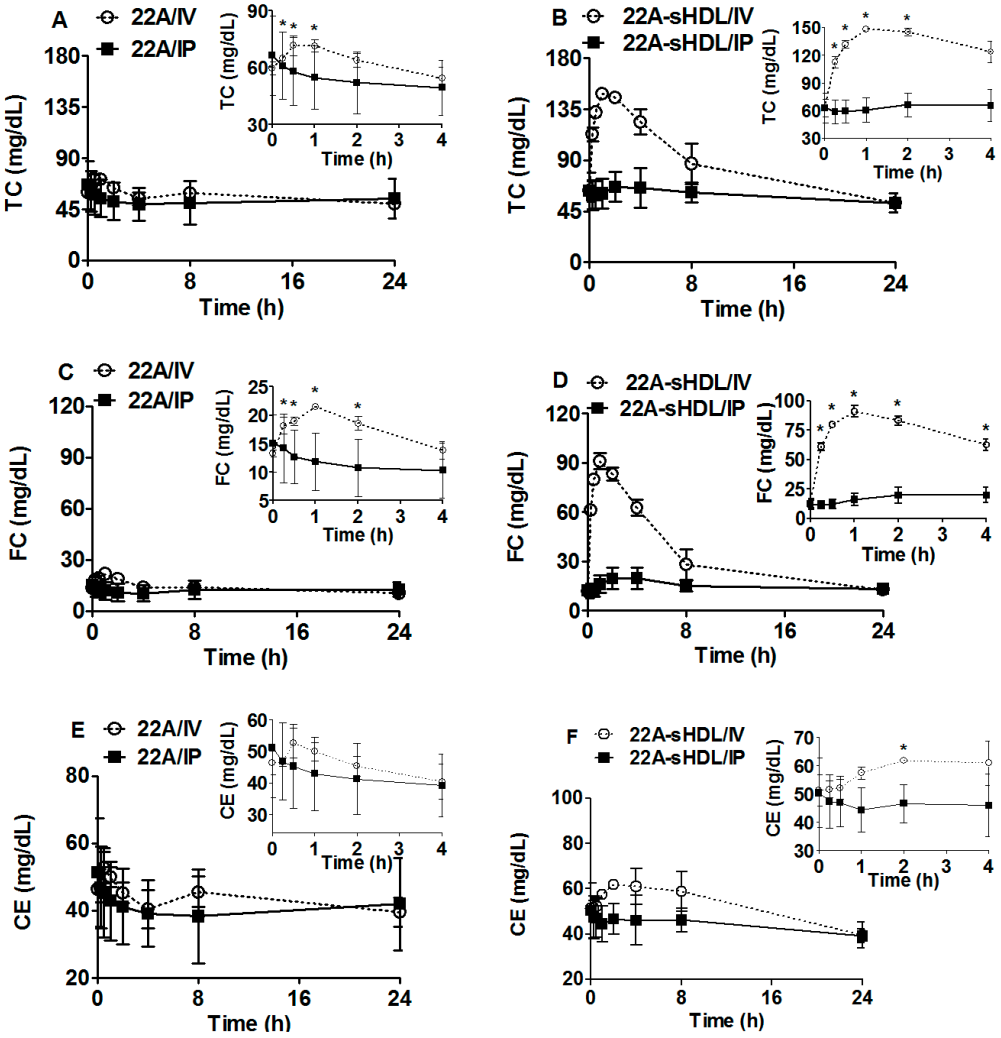

Figure 4. Pharmacodynamic assessment of sHDL therapeutics after IV or IP administration of lipid-free 22A peptide or 22A-sHDL. Mobilization of total TC (A and B), FC (C and D) and CE (E and F) after injection of 75 mg/kg of 22A peptide solution (A, C and E) and 22A-sHDL (B, D and F). (*) denotes statistical significant differences of TC, FC or EC changes compared with their pre-dose levels with p-values of at least < 0.05.

Figure 5:

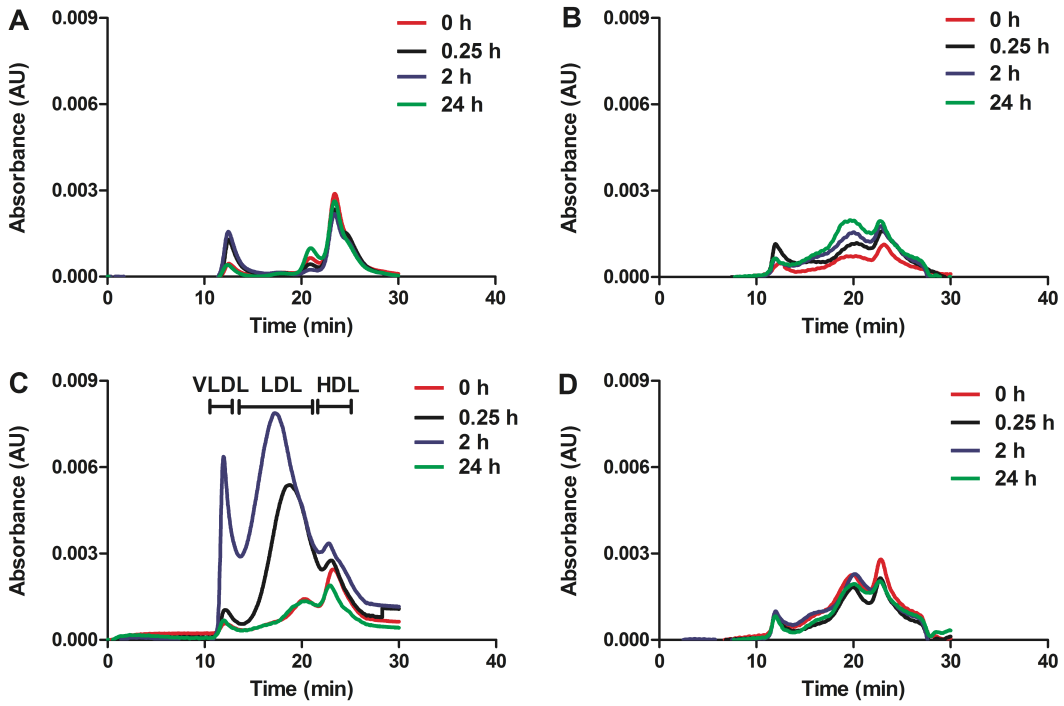

Figure 5. The cholesterol distribution between VLDL, LDL and HDL lipoprotein fractions following IV (A) or IP administration (B) of 22A peptide solution or IV (C) or IP administration (D) 22A-sHDL.

Figure 6:

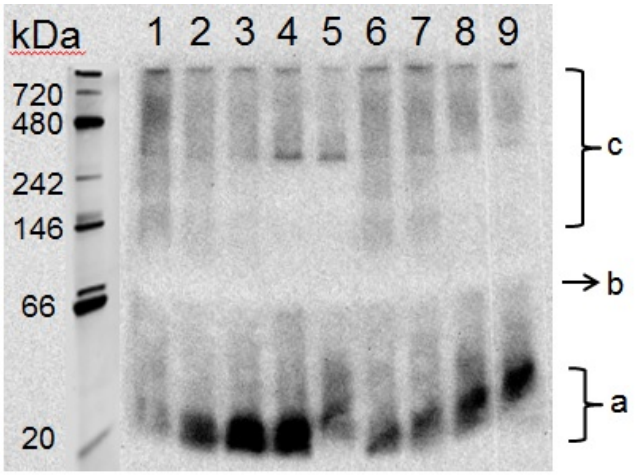

Figure 6. Free apoA-I and various subclasses of HDL were separated by 1-D native page electrophoresis and visualized by western blot using anti-apoA-I antibody. Lane 1 was the control serum, lane 2, 3, 4, 5 represented 0.15, 0.5, 1 and 3 mg/ml of 22A and lane 6, 7, 8, 9 represented 0.15, 0.5, 1 and 3 mg/ml 22A-sHDL, respectively. Labels a, b and c refer to the approximate positions of lipid-poor apoA-I, small pre-β HDL particles and large α-HDL particles.

Figure 7:

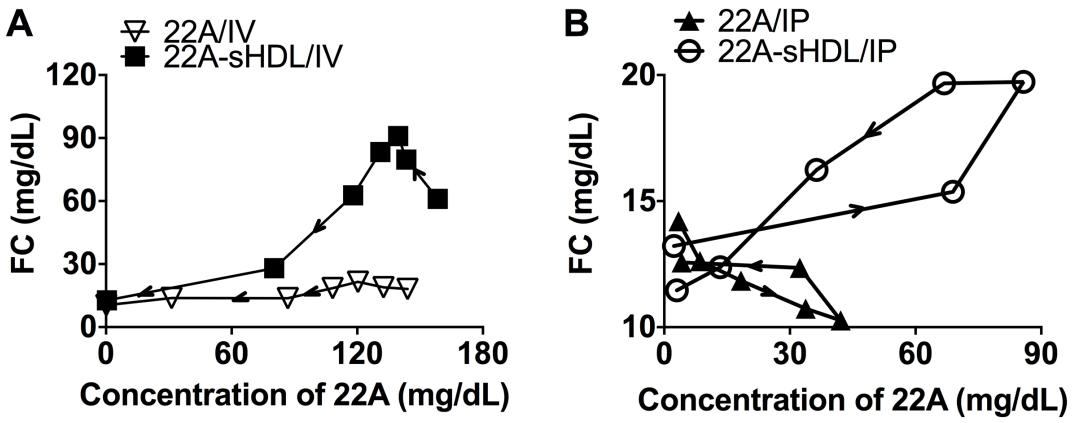

Figure 7. Plot of the relationship between 22A serum concentration and FC increase at individual time points following IV (A) or IP (B) administration of 22A peptide solution or 22A-sHDL at dose of 75 mg/kg.